TUTDoR

Adsorptive removal of Fe and Cd from the textile wastewater using ternary bio#adsorbent: adsorption, desorption, adsorption isotherms and kinetic studies.

Item Type	Article
Authors	Agboola, Oluranti;Nwankwo, Oluebube Jennifer;Akinyemi, Felicia Akinnike;Chukwuka, Jesica Chiderah;Ayeni, Augustine Omoniyi;Popoola, Patricia;Sadiku, Rotimi
Publisher	Springer and Discover
Rights	Attribution-NonCommercial-ShareAlike 4.0 International
Download date	2025-09-10 19:27:06
Item License	http://creativecommons.org/licenses/by-nc-sa/4.0/
Link to Item	https://hdl.handle.net/20.500.14519/1620

Research

Adsorptive removal of Fe and Cd from the textile wastewater using ternary bio-adsorbent: adsorption, desorption, adsorption isotherms and kinetic studies

Oluranti Agboola[1] · Oluebube Jennifer Nwankwo[1] · Felicia Akinnike Akinyemi[1] · Jesica Chiderah Chukwuka[1] · Augustine Omoniyi Ayeni[1] · Patricia Popoola[2] · Rotimi Sadiku[2]

Abstract

Ternary bio-adsorbent was synthesized by using sisal fiber as a base with the integration of conductive polymer; poly-aniline (PANI), supported with zero-valent iron nanoparticles by chemical activation with potassium hydroxide. The activation temperature impact on adsorption properties of Sisal fiber composite activated carbon was studied. The activation temperatures had a major effect on adsorption process as 100% removal efficiency was attained at 800 °C activated temperature. Scanning electron microscopy (SEM) was used for surface analysis of the adsorbent. Adsorption isotherms (Langmuir, Freundlich and Temkin) were examined and the negative values of $1/n_F$ demonstrated that the adsorption data does not match with Freundlich model for chemisorption. The pseudo second order and Elovich kinetics correlation coefficients for the retention of Fe and Cd to solid-phase interface at SF-800/NP/PANI (C) offered a better correlation for the bio-adsorption of Fe and Cd than pseudo first order kinetic. However, the pseudo second order kinetic attained a surpassing interaction for the bio-adsorption of Fe (0.989) than Cd (0.966); while the Elovich kinetic attained a surpassing interaction for the bio-adsorption of Cd (0.975) than Fe (0.945). The recovery and recycling stability of the bio-adsorbent composites were studied.

Keywords Textile industrial wastewater · Heavy metals · Bio-adsorbent composite · Adsorption isotherm · Kinetics · Desorption and regeneration

1 Introduction

Industrial wastewater is considered as a thrown away aqueous ensued from chemicals that have been dissolved in water, usually, in the course of the utilization of water in industrial processes or activities that involves cleaning, which occurs along with industrial processes [1]. Industrial wastewaters are more difficult to manage than residential waste. Industrial wastewater composition varies by industry [2]. Textile factory effluent dyes are considered the main cause of water

✉ Oluranti Agboola, funmi2406@gmail.com; oluranti.agboola@covenantuniversity.edu.ng; ✉ Felicia Akinnike Akinyemi, akinnike.akinyemi@covenantuniversity.edu.ng; Oluebube Jennifer Nwankwo, Oluebubejennifer20@gmail.com; Jesica Chiderah Chukwuka, jessicachiderah@gmail.com; Augustine Omoniyi Ayeni, augustine.ayeni@covenantuniversity.edu.ng; Patricia Popoola, popoolaapi@tut.ac.za; Rotimi Sadiku, sadikur@tut.ac.za | ¹Department of Chemical Engineering, Covenant University, Ota, Ogun State, Nigeria. ²Department of Chemical Metallurgical and Materials Engineering, Tshwane University of Technology, Pretoria, South Africa.

pollution in the environment. Surface water contains highly carcinogenic dyes and degradation products [3]. Hence, textile effluents must be treated before they are discharged into the water supply. The way dyes move and disperse in water have been investigated widely over the last three decades due to their toxic effects on humans, plants, animals, and aquatic organisms [4]. Nearly 25% of dye is been discharged in textile industries, and 2–21% of that amount is been discharged into quite a few environmental constituents via a direct process method. Due to the color of the dyes, aquatic life has a hard time getting enough sunlight. Because dyes have such a long half-life period, their noxious effects have gotten out of hand [5]. Dyes linger in the environment for a long time because there is no acceptable treatment process. As a result, it is difficult to decolorized effluents once released into the aquatic environment.

The most important methods for removing noxious waste from wastewater are reverse osmosis, precipitation, ion exchange and adsorption, among others. Among these techniques, the adsorption technique is adaptable and widely utilized for heavy metal removal [6]. Water and wastewater treatment have typically used activated carbon as their preferred adsorbent. Activated carbon (AC) can be gotten from different kinds of agricultural materials such as orange peels, coconut shells, walnut shells, cashew nuts and sisal fiber. The incomparable adsorptive properties of activated carbon (ACs) synthesized from sisal fiber ensued from its porosity; typically, such properties are accredited to their distinctive pore distribution pattern, high durability, recyclability and their large internal surface area [7]. Sisal Fibre (*Agave sisalana*), which is one of the sources for producing AC, is taken out from the leaves of *Agave sisalana*. This leaf is a vital source of fibres for composites on account of its biodegradability, high tensile strength and adaptability [8]. It is considered a fibre that is highly rich in cellulose; hence, comprises lignin and hemicellulose [9].

Synthetic polymer precursors are typically employed for producing AC when impure low-inorganic carbon materials are essentially needed [10]. Polyethylene terephthalate (PET) offers an outstanding precursor due to its high carbon content (about 62.5 wt%). In addition, its conversion to activated carbon provides serves as a means of combating polymer wastes; however, the utilization of PET for such a purpose produces low pyrolysis yield [10]. Conducting polymer is a novel class of organic substance that has previously been discovered for their remarkable physicochemical and electrical properties. The most popular forms of conducting polymers include polyaniline, poly(3,4-ethylenedioxythiophene), poly-pyrrole, poly-furan, poly(*p*-phenylenevinylene), polythiophene and their derivatives. Chemical and biosensors, recharge-able batteries, flexible transparent displays, photovoltaics, photocatalysts, energy storage, medicinal applications, and environmental cleanup are just a few of the possibilities for conducting polymer [11].

Polyaniline (PANI) is a polyaromatic amine that is chemically easy to make from Bronsted acidic aqueous solutions. It is one of the most promising conducting polymers, and it has been noticed a lot in recent years owing to its stability in the environment, cheap raw material costs, readily available monomer, good physicochemical properties, doping feasibility and ease of synthesis [12]. Polyaniline has been widely investigated for the improvement of adsorbents through synthetic alteration, doping, and the creation of composites. The presence of active groups, to be explicit amine, an imine, which teams up with molecules of various debasements present in polluted water, fits the normal usage of polyaniline as an adsorbent in wastewater treatment [13]. Furthermore, the use of PANI for adsorption has essentially credited to amine and imine polyfunctionalities that are present in PANI [14], this gave PANI the capability of removing pollutants owning to complexation and ion exchange [15]. Zare et al. [16] utilized polyaniline for the adsorption cycle for the elimination of cationic and anionic dyes from a fluid medium [16].

Nanomaterials are generally studied for their multi-useful applications in the food business, medication, and horticul-ture [17]. They certainly stand out for utilizing an adsorption cycle to disinfect water. The utilization of nanoparticles as a productive adsorbent is because they have higher surface regions than bulk particles on a mass basis, and they can be changed with different chemical groups to expand their substance partiality toward target compounds [18]. The improve-ment of nanocomposites has provoked logical and modern curiosity lately because of a few headways made conceivable by consolidating polymers and different adsorbents. Nanocomposites can likewise show extraordinary plan prospects, giving huge advantages in the making of practical materials with explicit properties for explicit applications [19].

Recent advancement in the employment of adsorbent for treating textile wastewater have depicted that hybrids adsorbents are more effective for treating wastewater. Lei et al. [20] used waste Polyacrylonitrile fiber (PANF) for effec-tive adsorption of dye. The synthesized fiber adsorbents were used for the removal of anionic dye. The synthesized fiber exhibited outstanding adsorption efficiency than a common adsorbent [20]. Badawi and Zaher [21] investigated the likelihood of employing hybrid system of treatment (coagulation/flocculation, adsorption and filtration processes) for treating textile wastewater. A study on the economic assessment was done in order to evaluate the commercial application of the system. All data attained confirmed the efficacy of employing the hybrid integrated system of treatment [21]. Wang et al. [22] employed in situ polymerization technique to synthesized a Chinese yam peel–PPy composite (CYP–PPy) and attained a high adsorption efficacy for the elimination of Congo red (CR) dye from aqueous

media. At equilibrium time of 20 h, 98.9% removal efficacy was considerably attained [22]. Shaki [23], studied a series of acid dyes removal by means of polyacrylamide/iron sulfate (PAM-FeSO$_4$) adsorbent. The study showed that the adsorbent possess a satisfactory adsorption capacity for the elimination the Orange II and Sunset Yellow.

The surface coating of PANI on fibrous materials is well thought-out to be a prospective technique for improving the short processability and the creation of polyaniline aggregate [24, 25]. Sisal fiber has attracted special consideration as reinforcement phase for many polymeric resin composites [26]. It has distinctive characteristics like strong mechanical property and coarse surface [27], which enable its appropriateness to coat the surface of polyaniline for the treatment of wastewater [24].

The motivation for using zerovalent iron nanoparticle was its favourable characteristics like high reactivities [28], high specific surface area [29] and high adsorption capacity for heavy metals [30]. And the motivation for using sisal fiber is its high content of cellulose and hemicelluloses properties which offer high adsorption capacities. Polymer own irreplaceable physical properties on account of their large molecular masses when equated to small molecule compounds like viscoelasticity, high elasticity, toughness, and the propensity to form amorphous and semi-crystalline structures in place of crystalline structures [31]. Hence, the significant of these use of this bio-adsorbent composite is its exceptional metal ion adsorbents as a result of the excellent properties such as large surface area, abundance of active site and tunable pores that will be attained from the three material used to synthesized the composite. This work seeks to assess the removal of metals ions from textile industry wastewater employing ternary bio-adsorbent synthesized by using sisal fiber as a base with the integration of conductive polymer; polyaniline (PANI), supported with zero-valent iron nanoparticles (SF/NP/PANI). The ability of the bio-adsorbent composites to be recycled for adsorption of heavy metals was examined.

2 Materials and methods

2.1 Materials and material pre-treatment

Sodium borohydride, ferrous sulfate, polyaniline and ethanol were procured from Sigma Aldrich. All the chemical reagents employed in this experiment were of laboratory reagent grade. The sisal fiber was gotten from Ota market in Ogun state. It was cut into 2 mm size. The glassware and plastic ware utilized in the course of the experimental and analytical work were rinsed three times with distilled water. The sisal fiber was rinsed in distilled water to eliminate contaminants and impurities. The washed sisal fiber was put in the electric oven for 1 h 30 min for 110 °C to eliminate any residual moisture. The dried sample was wrapped in a foil before carbonization.

2.2 Synthesis of zero valent iron nanoparticle

Zero valent iron nanoparticle was prepared via chemical reduction method. This method utilized a 1:2 proportion of sodium borohydride (NaBH$_4$, 0.2 M, 50 mL) to ferrous sulfate heptahydrate (FeSO$_4$·7H$_2$O, 0.5 M, 100 mL). 3.97 g of sodium borohydride was dissolved in 50 mL of distilled water and 13.9 g of ferrous sulfate heptahydrate salt was disintegrated in 100 mL of distilled water and combined as one, it was mixed constantly on a magnetic stirrer at ambient temperature (25 °C) for 5 min [32]. During the reduction reaction, variety changes quickly from clear caramel to dark with the development of colloidal precipitate. The solution which contains the magnetic iron nanoparticles was separated by employing a filter paper, after separation, the precipitate was washed twice with distilled water for the elimination of excess sodium borohydride and then with ethanol three times. The washed precipitate was transferred to an electric oven and dried at 100 °C for 1 h producing the nanoparticle [32].

2.3 Carbonization and activation of the carbon

The dried sisal fiber was wrapped in a foil and put into a stainless cup before entering the muffle furnace. The sisal fiber was carbonized in the automated muffle furnace in the absence of air at 400 °C. The samples were grinded with a mortar and pestle, after which it was accurately weighed and chemically activated with potassium hydroxide at the impregnation ratio of 1:1. The mixture was impregnated and set aside for 24 h at ambient temperature for the

Table 1 Adsorbent preparation ratio

S/N	Sisal fiber (SF) (g)	Zero-valent nanoparticle (NP) (g)	Polyacrylonitrile (PANI) (g)
A	3.6	0.025	0.025
B	3.6	0.1	0.04
C	3.6	0.4	0.01

Table 2 Experimental conditions

S/N	Experimental ID	Activation temperature (°C)	Dosage (g/80 mL)	Time (min)
1	SF-700/NP/PANI (A)	700	±4	10–60
2	SF-700/NP/PANI (B)	700	±4	10–60
3	SF-700/NP/PANI (C)	700	±4	10–60
4	SF-800/NP/PANI (A)	800	±4	10–60
5	SF-800/NP/PANI (B)	800	±4	10–60
6	SF-800/NP/PANI (C)	800	±4	10–60

purpose of allowing proper contact. The samples were then transferred to crucibles and dried in the electric oven for 2 h 30 min at 110 °C. It was thermally activated in the furnace at two temperatures of 700 °C and 800 °C for 2 h respectively. It was transferred to Whatman filter paper for the purpose of filtration, and the paste was constantly rinsed with distilled water until it attained a neutral pH value. The sample was transferred to the oven to be dried to a constant weight after which it was stored in an airtight polythene bag [33].

2.4 Batch adsorption experiment

The bio-adsorbent composite preparation dosage for the batch experiment is shown in Table 1. The textile waste-water was analyzed to find the concentration of cations and the cations with the high concentrations were chosen for adsorption experiment. From the atomic adsorption spectroscopy (AAS) results, Cadmium (Cd) (0.0264 mg/L) and Iron (Fe) (0.9403 mg/L) have a very high concentration in the textile wastewater. The pH value of the textile wastewater used for the study was 6.95. The pH was measured for the wastewater sample using a pH-meter (HI2209 bench top pH meter) purchased from Hanna Instruments, Wood socket RI USA. The pH meter was calibrated with two pH buffer standards and the adsorptions of Fe and Cd were carried out as follows: different parameters like activation temperature, adsorbent dosage and time were varied. The textile industrial wastewater was treated using SF activated carbon synthesized at two different activation temperatures (700 °C and 800 °C). Composites of AC were formed by integrating different ratios of the zero-valent ion nanoparticle and polyacrylonitrile into the synthesized SF activated carbon. A digital magnetic stirrer was employed to mix the solution in the batch adsorption process at a constant speed of 120 rpm and a constant pH of 5. The effect of adsorbent dosage (3.65, 4.01 and 4.1 g) was observed for the removal efficiency of Cd and Fe. The solution was filtered with Whatman filter paper and the filtered solution was subjected to AAS to determine target metal concentration. Two factors were used for the experiment which are controlled independent variable (time and activation temperature); while the dependent variable is the adsorption removal efficiency. Table 2 shows the conditions for the batch adsorption process which was manually designed on account of cost factor. The percentage removal efficiency (%R) of Fe and Cd is represented by utilizing Eq. 1 [34].

$$\%Removal\ Efficiency = \frac{C_i - C_f}{C_i} \times 100 \qquad (1)$$

where C_i (mg/L) and C_f (mg/L) are the metal ions concentration before and after adsorption experiments at time t.

2.5 Characterization

The structural configuration of the composite adsorbents was done by employing Scanning Electron Microscopy (SEM). It is an instrument that is commonly utilized for viewing the microstructure of composite adsorbents [35]. The equipment employed to access the surfaces of the samples was a TESCAN, furnished with Oxford instrument X-Max for the study of morphology. The SEM measurement was conducted by revealing the surface of the bio-adsorbent composites to a beam of electrons in vacuum at a specific accelerating voltage of 15 kV. The bio-adsorbent composites were died and mounted rigidly on a double-sided carbon tape to prepare them the SEM studies. The SEM study was done by exposing the samples to an electron beam. The EDS spectra was done to determine the samples' elements. ImageJ, a software from the National Institute of Mental Health, Bethesda, Maryland, USA was employed for the study of the pore size distribution. The SEM images observed on the microscope were converted into digital images to be analyzed using ImageJ which was utilized to measure the porosity of the bio-adsorbent composites. The ImageJ will also be employed to threshold the images for the purpose of visualizing the pores and attained the specific surface area.

2.6 Adsorption isotherms

In order to validate the percentage removal efficiency of the adsorption process and to further seek the adsorption parameters that verify the adsorption removal efficiency in the course of the adsorption process, Langmuir, Freundlich and Temkin isotherm models were studied. These adsorption isotherm models were used to describe a suitable fit with experimental data that provide a good correlation coefficient [36, 37]. The utilization of the adsorption isotherm to characterize the process of adsorption was assessed through the correlation coefficient value (R^2). The Langmuir isotherm presumes that the bio-adsorbent composites possess a homogeneous adsorbent surface, having the monolayer covered by the adsorbates and equality of the adsorption activation energy for each molecule on the surface [38]. Equation 2 gives the linearized expression of Langmuir adsorption isotherm. An important characteristics of the Langmuir isotherm is demonstrated with regards to a dimensionless constant known as separation factor/equilibrium parameter R_L, represented by Eq. 3. The impact of isotherm shape on whether or not the adsorption is favourable or not was assessed using Eq. 2 [39].

$$q_e = \frac{q_0 K_L C_e}{1 + K_L C_e}$$ (2)

$$R_L = \frac{1}{1 + K_L C_0}$$ (3)

In these equations C_e represents the concentration of equilibrium of Fe and Cd in (mg/L), q_e represents the quantity of Fe and Cd adsorbed per unit mass of adsorbent (mg/g). q_m and K_L respectively represent Langmuir constants connected to the peak adsorption capacity and energy of adsorption. In addition, C_O (mg/L) represents the initial concentration of Fe and Cd and K_L (L/mg) represents the Langmuir constant associated with the adsorption of energy. R_L designates the shape of the isotherms to be either unfavorable ($R_L > 1$), linear ($R_L = 1$), favourable ($0 < R_L$).

The importance of Freundlich Adsorption Isotherm model is to present the ratio of adsorbate adsorbed to the adsorbate concentration with respect to the solution concentration [40, 41]. Freundlich isotherm presumes adsorption takes place at heterogeneous adsorption sites and its consequence is multilayers formation [41] It can be mathematically expressed by the linearized equation given in Eq. 4 [41]:

$$\log q_e = \log K_F + \left(\frac{1}{n_F}\right) \log C_e$$ (4)

In this equation, q_e and C_e are as well-defined previously. K_F represents the multilayer adsorption capacity and n_F signifies the degree of dependence of adsorption with equilibrium concentration; having the range of $\frac{1}{n_F}$ between 0 and 1 which shows the extent of nonlinearity between concentration of solution and adsorption.

Temkin isotherm presumption is centered on the linear decrease in the heat of adsorption of all metal ions in the stratum with the surface coverage on account of adsorbent/adsorbate interactions. It is also assumed that the adsorption demonstrates even distribution of binding energies, until it gets to a certain binding energy peak [38, 42]. The model is presented in linear form using Eq. 5 [39].

$$q_e = \frac{RT}{b} ln\left(K_m C_e\right) \tag{5}$$

Which can be condensed to Eq. 6 [39].

$$q_e = \frac{RT}{b} lnC_e + \frac{RT}{b} lnK_m \tag{6}$$

In these equations, R is regarded as the universal gas constant in J/(mol K), T is regarded as the temperature in K. Where b stands for the Temkin isotherm constant associated with the heat of adsorption (J/mol), and K_m stands for the Temkin isotherm constant in L/g, which can be respectively estimated from the slope and the intercept of the linear graph of *qe* against ln(*Ce*).

2.7 Adsorption kinetics

One of the essential components that is used in estimating the adsorption rate is the adsorption kinetics examination; from which the mechanism of adsorption can be determined. Adsorption kinetics measure the adsorption uptake as a function of time while making the pressure or concentration constant and it is used to find the diffusion of adsorbate in the pores [43]. In this study, the adsorption kinetics were used to measure the release of textile wastewater solute from the aqueous media to the solute-phase interface of the bio-adsorbent composites with regards to time variation. For the purpose of studying and analyzing the adsorption kinetic; the pseudo-first order, pseudo second order and Elovich models were used. The pseudo-first order kinetic equation is represented by Eq. 7 [44].

$$\frac{dq(t)}{dt} = k_1 \left[q_e - q(t) \right] \tag{7}$$

Which in a simple form is represented by Eq. 8 [44].

$$q(t) = q_e \left(1 - e^{-k_1 t} \right) \tag{8}$$

In these equations, q_t represents the quantity of adsorbate adsorbed at time t (mg g^{-1}), q_e represents the adsorption capacity in the equilibrium (mg g^{-1}), k_1 represents the pseudo-first order rate constant (min^{-1}) and t is the contact time (min).

The pseudo-second order kinetic equation is represented by Eq. 9 [44].

$$\frac{dq}{dt} = k_2 \left(q_e - q \right)^2 \tag{9}$$

Which in a simple form is represented by Eq. 10 [44]

$$\frac{t}{q_t} = \frac{1}{k_2 q_e^2} + \left(\frac{1}{q_e} \right) t \tag{10}$$

where k_2 represents the pseudo-second order rate constant (g gm^{-1} min^{-1}), t is the contact time (min).

The Elovich equation has been utilized for chemisorption general application. Hence, the theory of Elovich has been satisfactorily employed to some chemisorption processes and literature found that it has covered an extensive span of slow rates of adsorption. In addition, this equation is usually binding for systems in which the adsorbing surface is heterogeneous, and is presented as Eq. 11 [45]:

$$\frac{dq_t}{dt} = a \exp \left(-bq_t \right) \tag{11}$$

In this equation, a and b are the parameters of the Elovich rate equation (initial adsorption rate and desorption constant). The constants could be attained from the slope and intercept of the graph of ln(t) versus q_t.
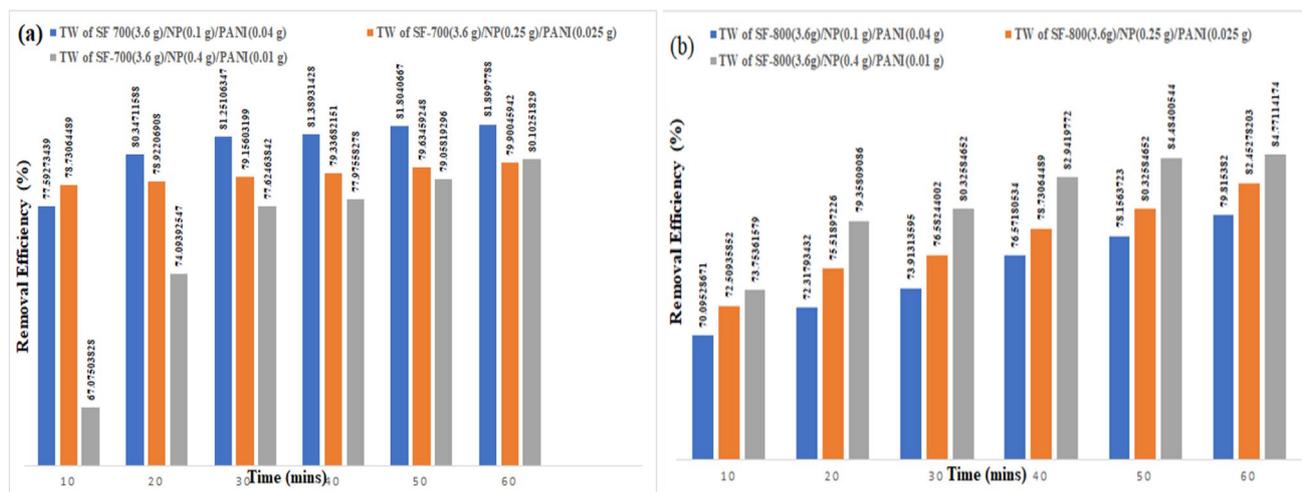
Fig. 1 Percentage removal efficiency of Fe @ **a** 700 °C of Sisal Fiber activation temperature; **b** 800 °C of Sisal Fiber activation temperature
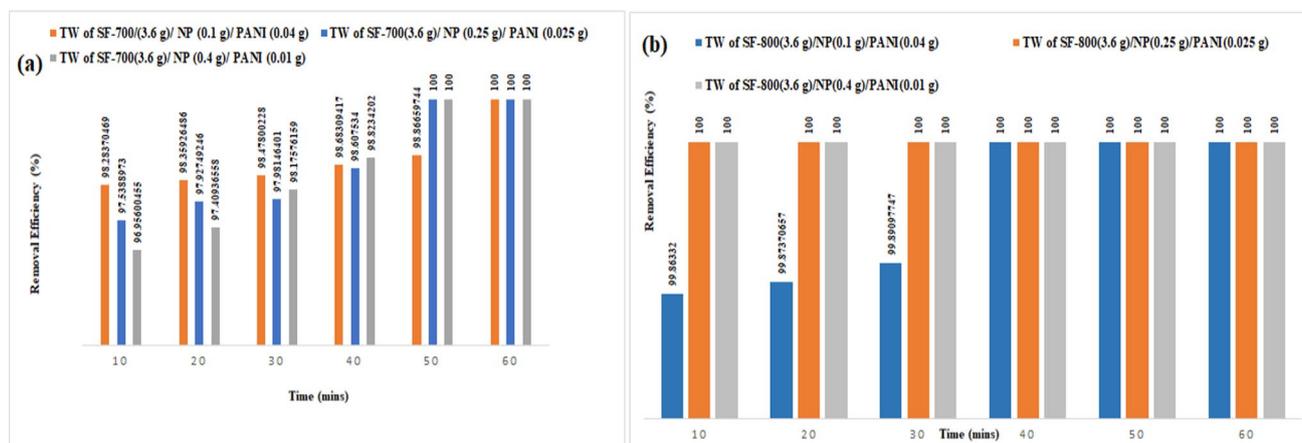

Fig. 2 Percentage removal efficiency of Cd @ **a** 700 °C of Sisal Fiber activation temperature; **b** 800 °C of Sisal Fiber activation temperature

3 Results and discussion

3.1 The removal rate

Activation temperature usually have remarkable effect on the pore structure and adsorption performance [46]. Figures 1 and 2 illustrate the percentage elimination efficiency of Fe and Cd at the activation temperature of 700 °C and 800 °C for the three different composites. As shown in Fig. 1, the percentage elimination of iron employing the three bio-adsorbent composites increased with an upsurge in time. However, the percentage removal of iron was lower when treated water (TW) of SF-700 (3.6 g)/NP (0.25 g)/PANI (0.025 g) and TW of SF-700 (3.6 g)/NP (0.1 g)/PANI (0.04 g) bio-adsorbent composites activated at temperature of 700 °C averagely attained 79.20% and 75.49% removal efficiency respectively, for iron. While an average of 80.71% removal of iron was attained when TW of SF-700 (3.6 g)/NP (0.1 g)/PANI (0.04 g) adsorbent activated at temperature of 700 °C was used. Nonetheless, averagely, TW of SF-800 (3.6 g)/NP (0.25 g)/PANI (0.025 g) and TW of SF-800 (3.6 g)/NP (0.1 g)/PANI (0.04 g) bio-adsorbent composites activated at temperature of 800 °C attained high removal efficiency of 77.69% and 75% respectively. While TW of SF-800 (3.6 g)/NP (0.4 g)/PANI (0.01 g) bio-adsorbent composite activated at temperature of 800 °C, averagely attained 80.1% after the adsorption process.

The performance of the bio-adsorbent composites was also observed for the erasure of cadmium. As displayed in Fig. 2, the percentage elimination of cadmium by employing the three bio-adsorbent composites also increased with

an upsurge in time. However, the percentage erasure of cadmium was lower when TW of SF-800 (3.6 g)/NP (0.25 g)/PANI (0.025 g), TW of SF-800 (3.6 g)/NP (0.1 g)/PANI (0.04 g) and TW of SF-800 (3.6 g)/NP (0.4 g)/PANI (0.01 g) bio-adsorbent composites activated at temperature of 800 °C averagely attained 98.7%, 98.8% and 98.7% removal efficiency respectively, for cadmium. It is important to note that 100% removal efficiency cadmium was observed for TW of SF-800 (3.6 g)/ NP (0.25 g)/PANI (0.025 g) and TW of SF-800 (3.6 g)/NP (0.4 g)/PANI (0.01 g) at 50 and 60 min. However, 100% removal efficiency of cadmium removal was attained with the three bio-adsorbent composite activated at 800 °C for all the time of adsorption (10–60 min) expect for TW of SF-800 (3.6 g)/NP (0.1 g)/PANI (0.04 g) bio-adsorbent composite that attained 100% removal efficiency at 40–60 min. This study shows that the synthesized bio-adsorbent composites is more suitable for the removal of cadmium from textile wastewater; however, bio-adsorbent composites activated at 800 °C are more suitable as they gave 100% removal.

These results show that the potassium hydroxide (KOH) is highly effective at 800 °C for the removal of iron and cadmium; however, cadmium has the highest removal efficiency for the bio-adsorbent composites. In addition, the variance in the adsorption performance could be correlated to their surface characteristics which is influenced by the activation temperature. This could also be as a result of the upsurge in materials' surface area with an upsurge in activation temperature; which resulted in the improvement of the porosity in the bio-adsorbent composites [47, 48]. Hence, the higher the surface area, the more pores expected to be developed in order to make available free active sites. In consequence, it possibly will make available higher likelihoods for the iron and cadmium molecules to be adsorbed on the surface of adsorbent's composites [49]. In addition, the high specific surface area establishes the existence of high amounts of –OH groups on the surface of the synthesized bio-adsorbent composites [50]. The advantages of the bio-adsorbent composite are the attainment of the large surface area that subsequently developed more pores that resulted to abundance of active site.

3.2 SEM, EDX and pore size study

The bio-adsorbent composites that gave the highest percentage removal efficiency for Fe and Cd were selected for SEM analysis to have a good surface analysis of the bio-adsorbent composites that offered good adsorption efficiency (adsorption composites prepared at 800 °C). Subsequently, all other investigations were studied at 800 °C. Hence, as a result of the data attained from percentage removal efficiency; SEM was done to examine the high-description micrographs of the bio-adsorbent composites. Figure 3 depicts that micrographs have diverse and tailorable shapes on account of the preparation ratio. The Figure shows that the micrographs clearly demonstrated bundle structure as a result of the preparation of AC by utilizing chemical activation; on account that activating agents have the capacity to easily having contact with the interior surface of material [51]. Furthermore, the three micrographs in Fig. 3 depicts a nanofibrillar structure achieved for the PANI synthesized with sisal fiber; hence, the bio-adsorbent composites are composed of interconnected nanofibers. Nevertheless, as the polymerization continues in the course of the synthesis, the attained composites become thicker and coarser ensuing from the creation of mostly irregularly shaped with aggregation of molecules [52]. In addition, Fig. 3 depicts a noteworthy variation in the morphology, particularly in size and pores. The SEM images of the bio-adsorbent composites confirmed that wide-ranging exterior surfaces with high porosity were formed at the activation point. It
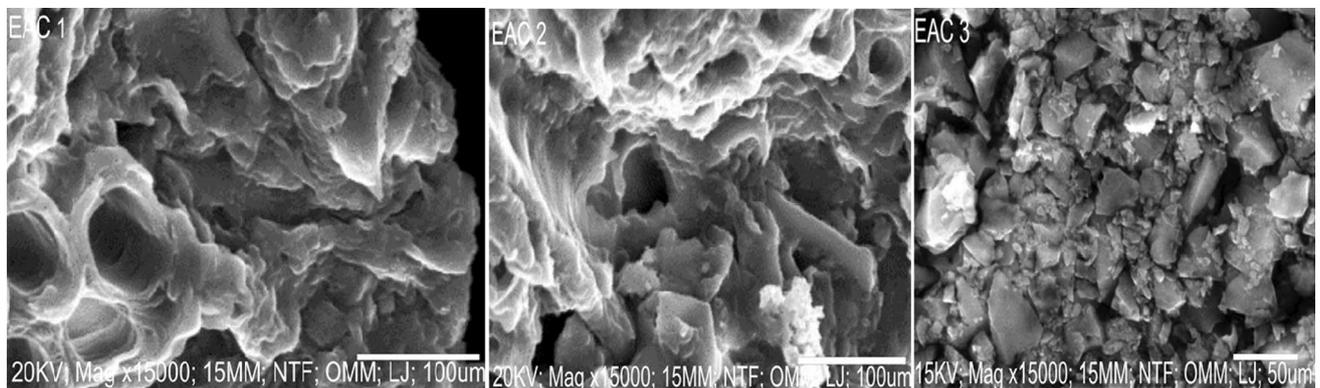

Fig. 3 Bio-adsorbent composite surfaces: (EAC1) SF-800 (3.6 g)/NP (0.1 g)/PANI (0.04 g); (EAC2) SF-800 (3.6 g)/NP (0.25 g)/PANI (0.025 g); (EAC3) SF-800 (3.6 g)/NP (0.4 g)/PANI (0.01 g)

was observed that the outer surfaces of the bio-adsorbent composites have high porosity. These pores ensued from the evaporation of chemical reagents in the course of carbonization allowing the spaces to be empty [53]. Furthermore, In Fig. 3, it was observed that samples' structures were rough with the (EAC3) having high aggregation of molecules. This singularity permitted the higher adsorption capacity of materials [54, 55]; hence, the efficiency of adsorbent increased (see Fig. 2). Through the study of the EDS shown in Fig. 4, It was observed that the main compounds in the bio-adsorbent composites are carbon and oxygen; this is because the amount of sisal fiber added into the composites is much higher than other component that make the composites.

The statistical distribution of the radius of the largest sphere that can fit inside a pore at a certain point is depicted in Fig. 5. The pore size distribution of bio-adsorbent composites has capacity to impact on the performance of the bio-adsorbent composites through the diffusion of adsorbate. The pore size of an adsorbent material is very vital for the access of the adsorbate species. Figure 5a confirmed what was observed in Fig. 3 with the variation in the morphology with respect to the pores. It confirmed that the bio-adsorbent composites possess wide-ranging exterior surfaces with high porosity. The grey area of Fig. 5b is confirmation of the pores in Fig. 3. In accordance with the International Union of Pure and Applied Chemistry (IUPAC), pore diameters of a material smaller than 2 nm are characterized as microporous [56]; hence, and retention of solutes in micropores. It was observed from the Fig. 5 that the three bio-adsorbent composites exhibited microporous size material with EAC1, EAC2 and EAC3 having average pore sizes of 0.046 nm, 0.043 nm and 0.019 nm respectively with a total surface area of 8.969 m^2/m^3, 6.975 m^2/m^3 and 4.640 m^2/m^3 respectively. Other data
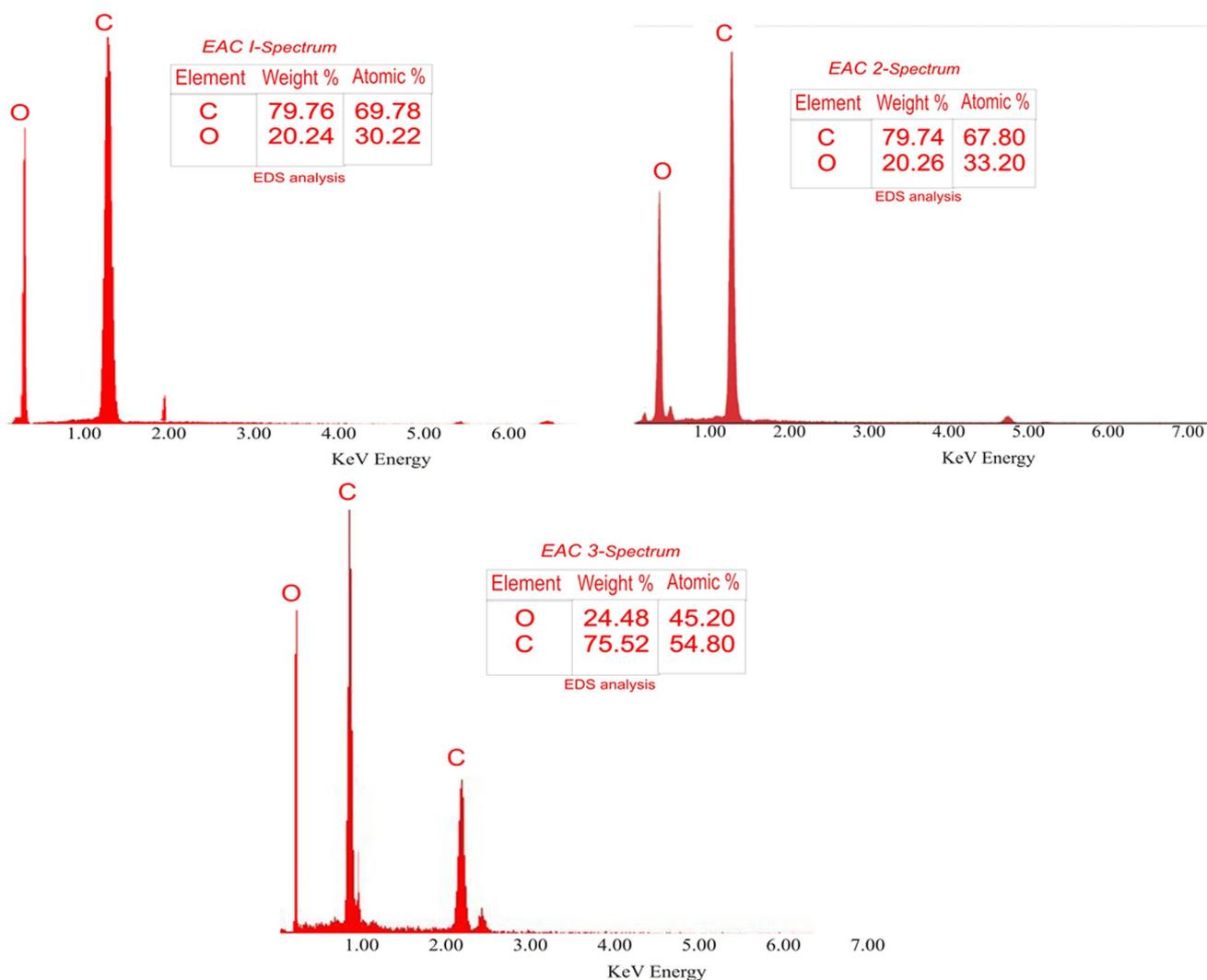

Fig. 4 EDS study of: (EAC1) SF-800 (3.6 g)/NP (0.1 g)/PANI (0.04 g); (EAC2) SF-800 (3.6 g)/NP (0.25 g)/PANI (0.025 g); (EAC3) SF-800 (3.6 g)/NP (0.4 g)/PANI (0.01 g)
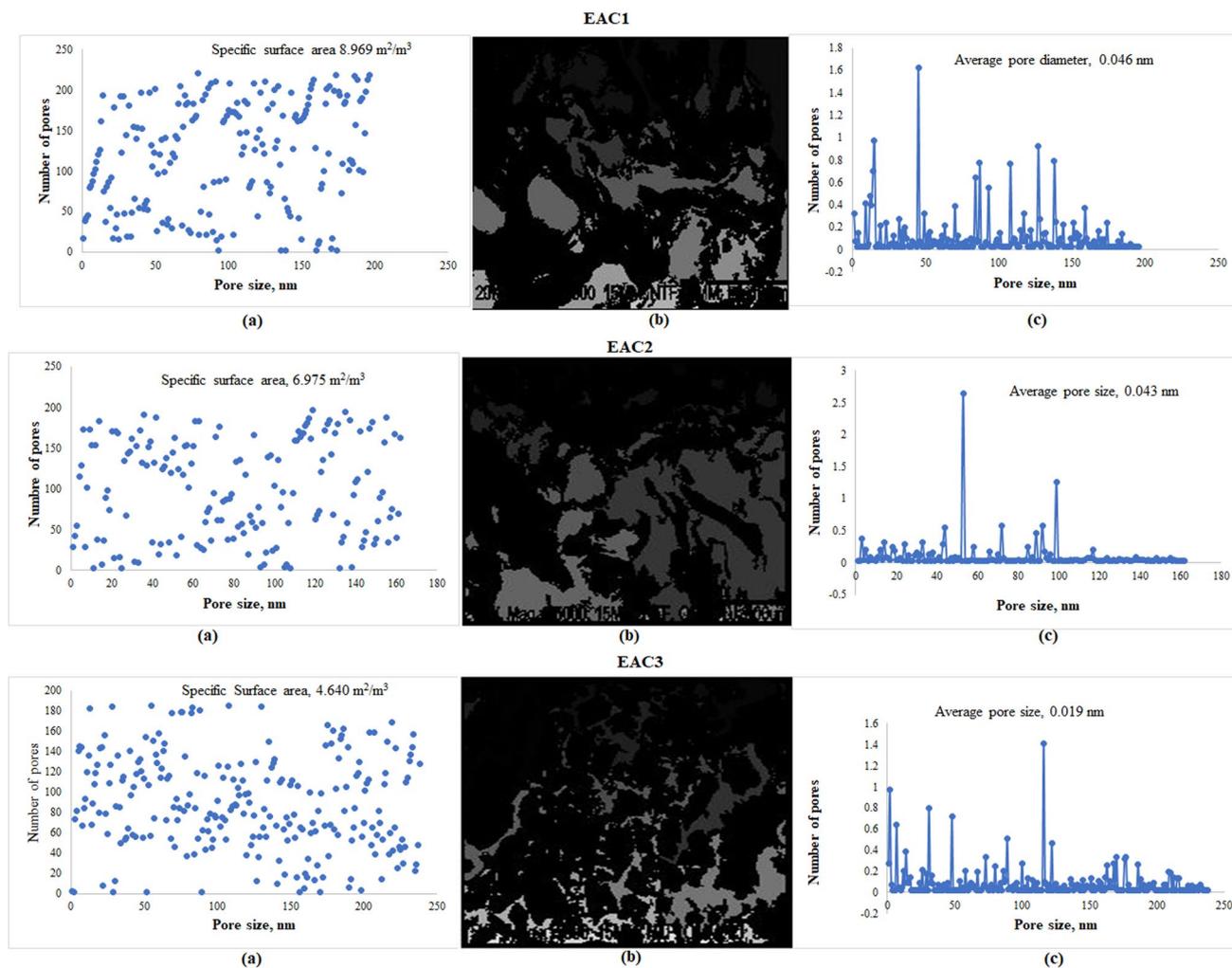
Fig. 5 Pore size distribution of: (EAC1) SF-800 (3.6 g)/NP (0.1 g)/PANI (0.04 g); (EAC2) SF-800 (3.6 g)/NP (0.25 g)/PANI (0.025 g); (EAC3) SF-800 (3.6 g)/NP (0.4 g)/PANI (0.01 g). **a** shows the number of pores with respect to various pores sizes, the grey area in; **b** is the confirmationof the pores while; **c** depicts high aggregation of molecules in the bio-adsorbent composites

such as mean, mode, median and feret are in the supplementary file. Furthermore, Fig. 5c, confirmed the high aggregation of molecules observed in Fig. 3.

3.3 Study of adsorption isotherms

The adsorption study was only done for SF-800/NP/PANI (C) adsorbent because a higher percentage removal efficiency was attained for the activation temperature of 800 °C. Langmuir, Freundlich and Temkin isotherm models examined are depicted in Figs. 6, 7, 8. Figure 6 is the representation of Langmuir isotherm for removal of iron and cadmium at 800 °C activation temperature. The values of q_m and K_L were calculated from the slope and are furnished in Table 3. The attained values of R_L are respectively 0.847 and 0.645 for Fe and Cd ions adsorption on SF-800/NP/PANI (C) sample at 800 °C activation temperature shows that the Fe and Cd uptake is favorable; as $0 < R_L$. The correlation coefficient is 0.9998 and 1 for Fe and Cd respectively at 800 °C. Hence, the correlation coefficient for the removal of Cd at obeyed Langmuir isotherm more than the correlation coefficient for the removal of Fe. However, the data shows the model is suitable for both Fe and Cd, indicating that the adsorption the metals on the bio-adsorbent composites was a chemical adsorption process, which was steady with the monolayer adsorption, as depicted in the Langmuir model [57].

Figure 7 is the representation of Freundlich isotherm for removal of iron and cadmium at 800 °C activation temperature. The Freundlich isotherm parameters, K_F and n_F are attained from the intercept and slope of the Fig. 7 (see Table 3). The correlation coefficients are respectively 0.9989 and 0.9858 for Fe and Cd at 800 °C. Hence, the correlation coefficient
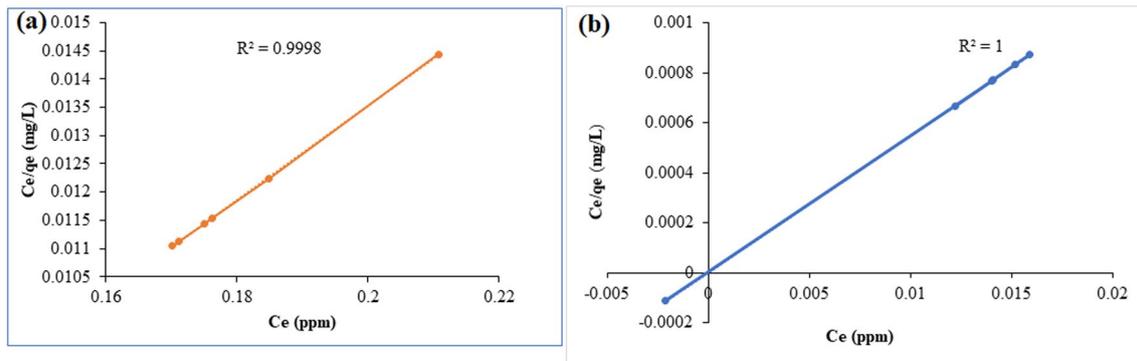
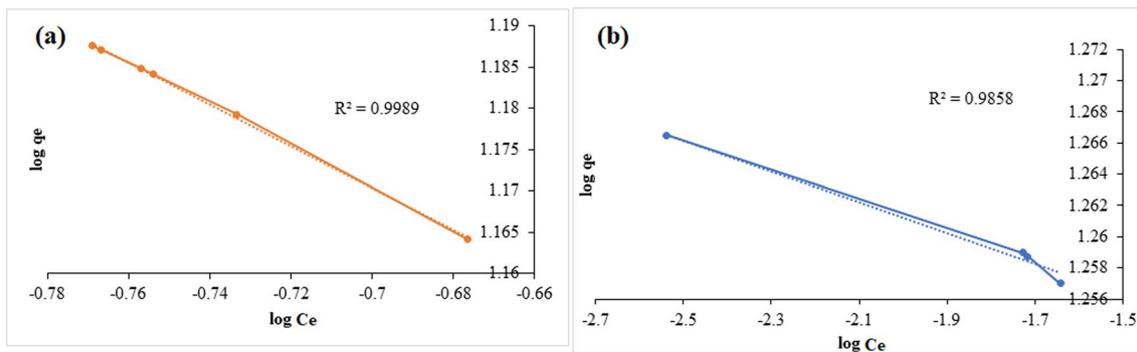**Fig. 6** Langmuir **a** Fe; **b** Cd @ 800 for SF-800/NP/PANI (C) sample

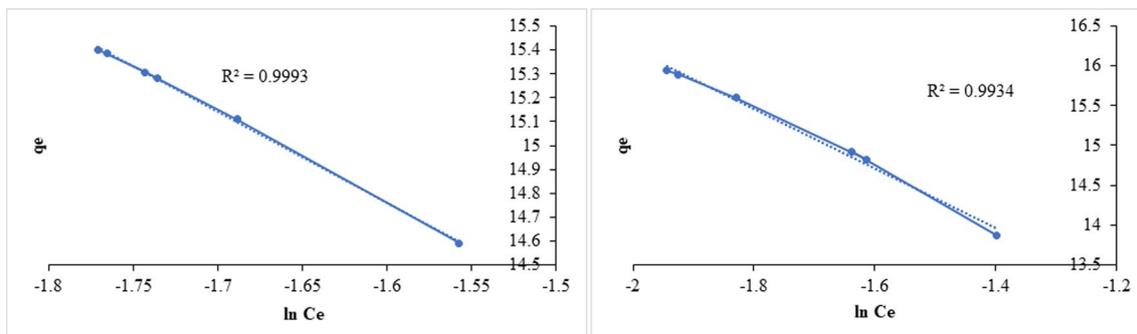**Fig. 7** Freudlich **a** Fe; **b** Cd @ 800 for SF-800/NP/PANI (C) sample

Fig. 8 Temkin **a** Fe; **b** Cd @ 800 for SF-800/NP/PANI (C) sample

for the removal of Fe show that the Freundlich isotherm was obeyed more for the removal of Fe than the removal of Cd. The Freundlich constant, n_F attained from the experiment are -0.2538 and -0.0153 at 800 °C for Fe and Cd respectively. Though the correlation coefficients are high; however, the negative values of $1/n_F$ indicates that the current adsorption data does not match with Freundlich model. Hence, the surface of adsorbent is non-heterogeneous with an exponential distribution of energy sites; in other words, it demonstrates an unfavorable physical process of adsorption of Fe and Cd [58]. This is on account that Freundlich constant is a characteristic of the correlative sorption capacity factor which is subsequently a characteristic of the magnitude of the adsorption and heterogeneity of the system [59]. In addition, it was recorded in a study that should the value of n_F appears less than unity, it infers that adsorption process is chemical which is a favorable chemical process [60, 61].

Figure 8 is the representation of Temkin isotherm for removal of iron and cadmium at 800 °C activation temperature; and the Temkin constants are estimated in Table 3. The correlation coefficients are 0.9993 and 0.9934 for Fe and Cd respectively at 800 °C. Therefore, the correlation coefficient for the removal of Fe 800 °C obeyed the Temkin isotherm

Table 3 The isotherm parameters for adsorption of metal ions @ 800 °C for SF-800/NP/PANI (C) sample

Activation temperature	Metals	Parameters	
800 °C	Fe	Langmuir	
		Q_{max}	11.185 (mg g^{-1})
		K_L	0.048 (L mg^{-1})
		R_L	0.847
		R^2	0.9998
		Freundlich	
		K_F	2.6985 (mg g^{-1})
		n_F	−0.2538
		R^2	0.9989
		Temkin	
		K_T	1.022
		b_T	254.34 (J mol^{-1})
		R^2	0.9993
800 °C	Cd	Langmuir	
		Q_{max}	18.181 (mg g^{-1})
		K_L	0.123 (L mg^{-1})
		R_L	0.645
		R^2	1.000
		Freundlich	
		K_F	3.4311 (mg g^{-1})
		n_F	−0.0153
		R^2	0.9981
		Temkin	
		K_T	1.037
		b_T	264.38 (J mol^{-1})
		R^2	0.9934

than the removal of Cd. The Temkin constants for the chosen sample [SF-800/NP/PANI (C)] observed in Table 3, show that the adsorption heat of Iron and cadmium adsorption on the chosen sample for adsorption study was restricted within 254.34–264.34 J/mol for the removal of Fe and Cd. This high degree of fitting with the models could aid in understanding the removal mechanism of Fe and Cd which will subsequently offer a good idea in improving the properties of the bio-adsorbent composites [57].

3.4 Study of adsorption kinetics

Just as the adsorption study was only done for SF-800/NP/PANI (C) adsorbent sample because a higher percentage removal efficiency was attained for the adsorbent at activation temperature of 800 °C; in the same vein, the kinetic study was only done for SF-800/NP/PANI (C) adsorbent sample. Three different adsorption kinetics (Pseudo-first order, Pseudo-second order and Elovich) study were employed to describe the rate of retention Fe and Cd to solid-phase interface at SF-800/NP/PANI (C) adsorbent sample (see Figs. 9, 10, 11). The parameters for the three kinetics studies obtained from the slope and intercept are furnished in Table 4. The pseudo first order kinetics correlation coefficients for the retention of Fe and Cd to solid-phase interface at SF-800/NP/PANI (C) are 0.0645 and 0.9775, respectively; which resulted to the conclusion that pseudo first order kinetic provides a poor correlation for the bio-adsorption of Fe and Cd (see Fig. 9). However, the linear plot of t/qt versus t depicts that there is an equitable confirmation between experimental and theoretical values (see Fig. 10). The correlation coefficients for the pseudo second order kinetics for the retention of Fe and Cd to solid-phase interface at SF-800/NP/PANI (C) are 0.989 and 0966, respectively; which led to the assumption that pseudo second order kinetic offered a better correlation for the bio-adsorption of Fe and Cd than pseudo first order kinetic. In addition, the plot of t/qt against versus t depicted a linear relationship shows that the pseudo-second-order kinetics is applicable for the study, and the equilibrium adsorption capacity, q_e, was calculated from Eq. (9). Furthermore, the correlation coefficients for Elovich kinetics for the retention of Fe and Cd to solid-phase interface at SF-800/NP/PANI
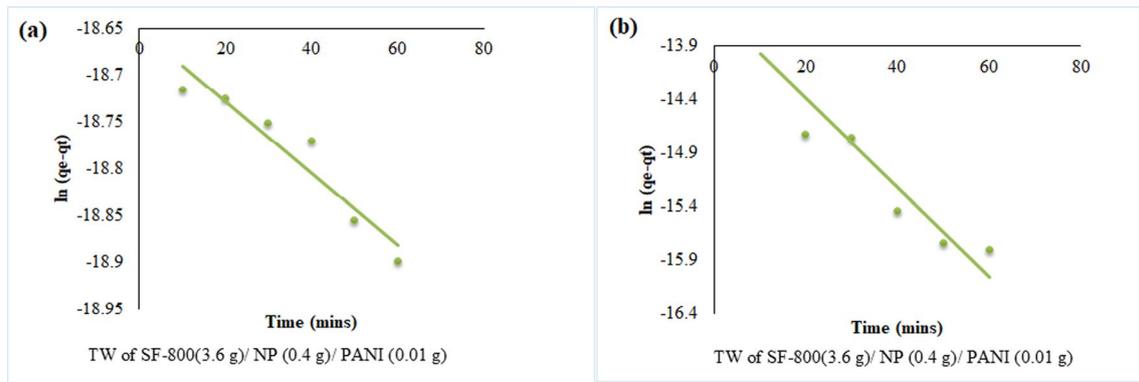
Fig. 9 Pseudo-first order kinetics for the adsorption of **a** Fe, **b** Cd ions onto SF-800/NP/PANI (C) adsorbent sample
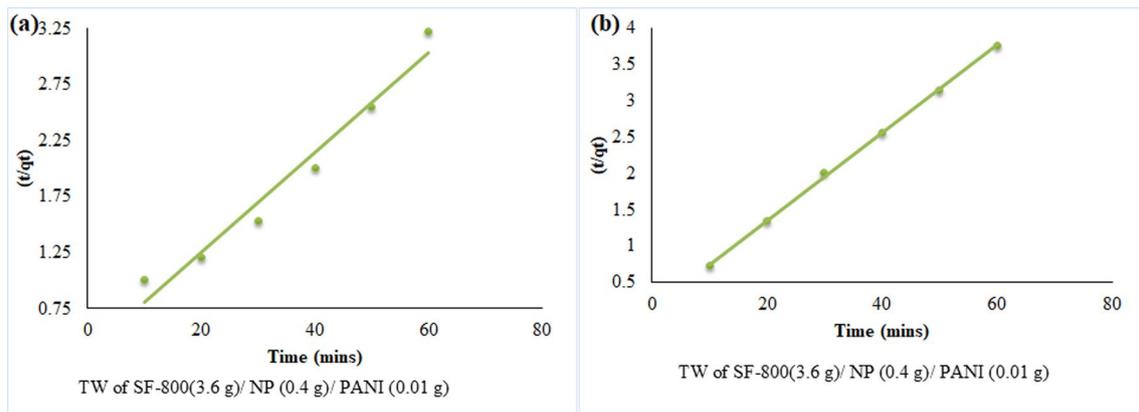

Fig. 10 Pseudo-second order kinetics for the adsorption of **a** Fe, **b** Cd ions onto SF-800/NP/PANI (C) adsorbent sample
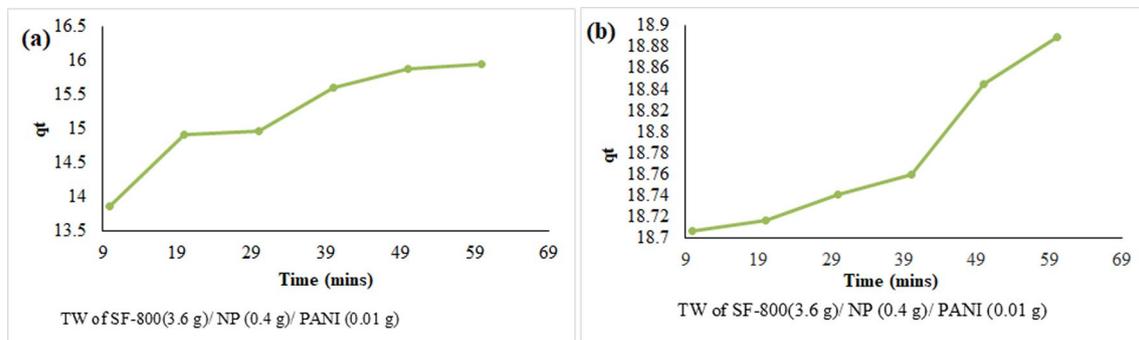

Fig. 11 Elovich order kinetics for the adsorption of **a** Fe, **b** Cd ions onto SF-800/NP/PANI (C) adsorbent sample

(C) are 0.945 and 0.975, respectively; which also resulted to the assumption that Elovich kinetic also offered a better correlation for the bio-adsorption of Fe and Cd than pseudo first order kinetic. Overall, the pseudo second order kinetic offered a better correlation for the bio-adsorption of Fe (0.989) than Cd (0.966); while the Elovich kinetic offered a better correlation for the bio-adsorption of Cd (0.975) than Fe (0.945) (see Table 4). These kinetic results have been influenced by the characteristic of the bio-adsorbent composites which include the point of zero charge, the pore size [62], cation exchange capacity, and the textile wastewater characteristics such as the pH [63], the hydrated ionic radius of metals and the complexation of metals.

Table 4 The kinetic parameters attained from the study	Activation temperature	Metals	Parameters	
	800 °C	Fe	Pseudo-first order	
			q_e (mg/g)	0.3365
			k_1	0.00424
			R^2	0.0645
			Pseudo-first order	
			q_e	16.53 mg/g
			k_1	0.02568
			R^2	0.989
			Elovich	
			α	12.86 g/mg
			β	1.632
			R^2	0.945
	800 °C	Cd	Pseudo-first order	
			q_e	0.15342 mg/g
			k_1	0.00019
			R^2	0.0775
			Pseudo-first order	
			q_e	26.54 mg/g
			k_1	0.02887
			R^2	0.966
			Elovich	
			α	16.58 g/mg
			β	1.167
			R^2	0.975

3.5 Desorption and regeneration study

The recovery and recycling stability of the solid adsorbents is considered one of the most significant features in practical applications for the removal of dye from industrial wastewater as such adsorbents will possess outstanding adsorption capacity and high desorption property that will decrease secondary pollution and the total cost [64]. Hence, the desorption experiments of the best-performed adsorbents at the end of 60 min adsorption were done to assess the recyclable potential. By employing the method of Yao et al. [65] and Wang et al. [64], the already utilized adsorbent prepared at 800 °C were washed using acidic ethanol as eluent; which serves as the carrier portion of the mobile phase for the adsorbed Cd molecules to be effectively desorbed. Cd was considered for recyclability study because 100% efficiency was attained with the adsorbent prepared at 800 °C [64, 65]. The outcome of treated wastewater (TW) for repeated adsorptions-desorption of two cycles are shown in Fig. 12, with TW of SR-800 (3.6 g)/NP (0.4 g)/PANI (0.01 g) having an average percentage removal of 96.55% and 95.60% for the first and second cycle respectively. TW of SR-800 (3.6 g)/NP (0.025 g)/PANI (0.025 g) have an average percentage removal of 95.84% and 94.25% for the first and second cycle respectively; while TW of SR-800 (3.6 g)/NP (0.1 g)/PANI (0.04 g) have an average percentage removal of 94.60% and 93.58% for the first and second cycle respectively. The adsorption capacity depicted that Cd adsorbed on adsorbent prepared at 800 °C decreased to some extent at the end of every cycle of adsorption–desorption process. However, the bio-adsorbent made at 800 °C can be employed repeatedly for the erasure of Cd from industrial wastewater treatment as the percentage removal of all the bio-adsorbent composites respectively attained over 94% and 93% percentage removal of Cd for the first and second cycles.

3.6 Analysis of the adsorption mechanism of ternary adsorbent for the wastewater

The surface characteristics of the ternary adsorbent, like surface area, pore size and functional groups have a significant role to play in the study of heavy metal analytes' capacity and adsorption mechanism [66]. One of the most imperative
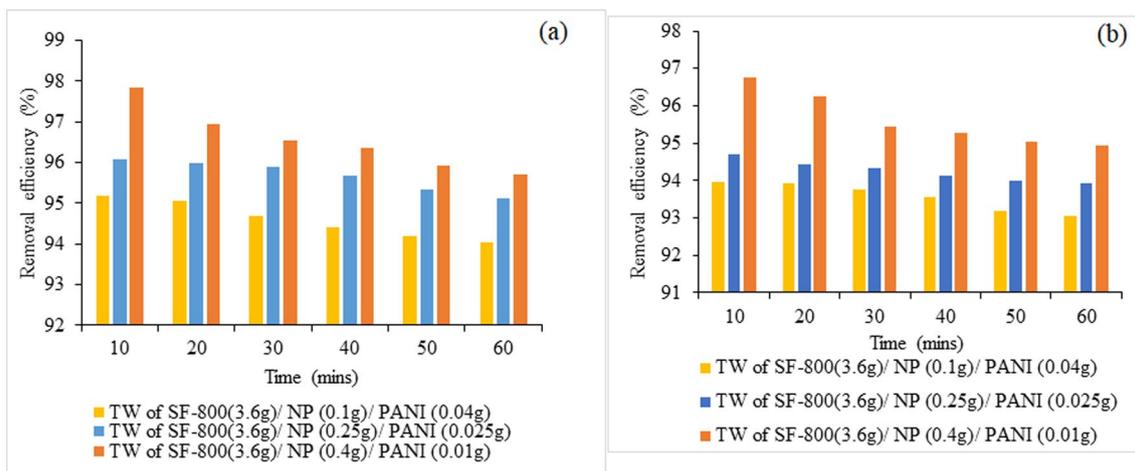
Fig. 12 Evaluation using SF-800/NP/PANI for the **a** first cycle and **b** second cycle of cadmium removal

factors that will govern the adsorptive mechanism of ternary adsorbent for metal ion adsorption is the ternary adsorbent configuration and its porous nature [67]. Figure 13 shows the adsorption mechanisms of ternary adsorbent for the erasure of Fe and Cd in textile wastewater; this is the demonstration of how this present study differs from previous studies. The ternary adsorbents have the capacity to upsurge the adsorption affinity for Fe and Cd by presenting Van der Waals interactions, hydrogen bonds, and or electrostatic interactions [68]. Other prospective adsorption mechanism possibilities for Fe and Cd adsorption on the ternary adsorbents includes:

i.   Surface complexation between Fe and Cd ions which is a process that ensues when multiple species combine on the surface of the ternary adsorbents also play an imperative role in the process [68].

ii. Electrostatic interaction between Fe and Cd and the surface of ternary adsorbents, which ensued on account of the ternary adsorbents surface possessing either a negative or positive charge to create an electrostatic attraction force that is accountable for drawing the oppositely charged Fe and Cd ions in the direction of the ternary adsorbents [69].
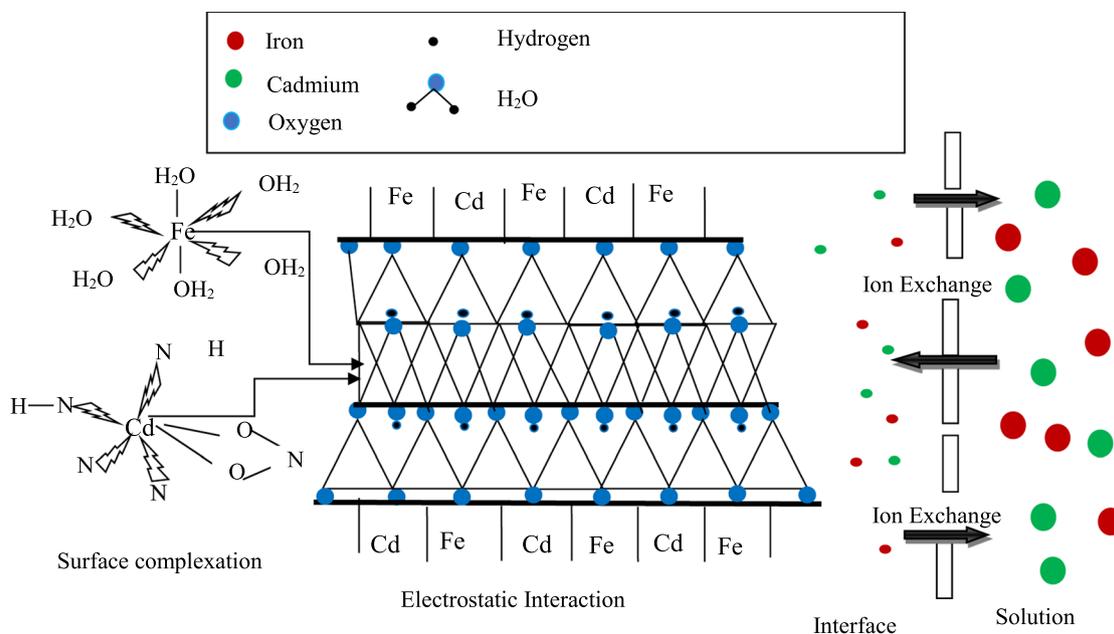

Fig. 13 Schematic representation for the adsorption mechanism of iron and cadmium by the ternary adsorbents

iii.   Ion exchange reactions between Fe and Cd ions and ternary adsorbents which ensued during the exchange process. In the course of the exchange process, the ions went through strong nonclassical polarization close to the solid–liquid interface under the influence of the surface electric field [70].

4 Limitation of the study

The limitation of the study was the utilization of Brunauer, Emmett and Teller (BET) for the determination of their pore size distribution, the pore volume and the total specific surface area that characterized the porosity of materials. In addition, three important factors which includes specific surface area, pore structure, and surface chemical functional group affects the adsorption capacity of biomass-derived activated carbon [71]; though this study studied the pore structure and pore surface area using ImageJ, however, chemical functional group was not studied.

5 Conclusion

Bio-material supported zero-valent iron nanoparticles and polyaniline was synthesized and used for the adsorption of Fe and Cd from textile wastewater. It was demonstrated that the bio-adsorbent composites are more suitable for the removal of cadmium from textile wastewater; however, bio-adsorbent composites activated at 800 °C are more suitable as they gave 100% removal for Cd. It was established in the batch adsorption studies; the activation temperature influenced the adsorption process. Also, the equilibrium was well fitted by the Langmuir isotherm model as the correlation coefficient is 0.9998 and 1 for Fe and Cd respectively at 800 °C. The kinetics demonstrated that the adsorption process agrees with the pseudo-second-order and Elovich model kinetics. The bio-adsorbent synthesized at 800 °C can be repeatedly utilized for the erasure of Cd from textile industrial wastewater treatment as the percentage removal of all the bio-adsorbent composites respectively attained over 94% and 93% percentage removal of Cd for the first and second cycles. The ternary bio-adsorbent synthesized in this study experiment could be a potential adsorbent in removing Cd from textile industrial wastewater treatment.

Data availability The authors declare that the data supporting the pore size distribution of this study obtained from ImageJ are available within the paper and its supplementary information files. Should any raw data files be needed in another format they are available from the corresponding author upon reasonable request. Source data are provided with this paper.

Code availability Not applicable.

Declarations

Competing interests The authors declare no competing interests.

References

1. Woodard, Curran I. 1—Evaluating and selecting industrial waste treatment systems. In: Woodard, Curran I, editors. Industrial waste treatment handbook. 2nd ed. Burlington: Butterworth-Heinemann; 2006. p. 1–28.
2. Pelissari C, Ávila C, Trein CM, García J, de Armas RD, Sezerino PH. Nitrogen transforming bacteria within a full-scale partially saturated vertical subsurface flow constructed wetland treating urban wastewater. Sci Total Environ. 2017;574:390–9.
3. Gaouar-Yadi M, Tizaoui K, Gaouar-Benyelles N, Benguella B. Efficient and eco-friendly adsorption using low-cost natural sorbents in waste water treatment. Indian J Chem Technol. 2016;23:204–9.
4. Khan TA, Dahiya S, Ali I. Use of kaolinite as adsorbent: equilibrium, dynamics and thermodynamic studies on the adsorption of Rhodamine B from aqueous solution. Appl Clay Sci. 2012;69:58–66.
5. Kahlon SK, Sharma G, Julka JM, Kumar A, Sharma S, Stadler FJ. Impact of heavy metals and nanoparticles on aquatic biota. Environ Chem Lett. 2018;16(3):919–46.
6. Tong KS, Kassim MJ, Azraa A. Adsorption of copper ion from its aqueous solution by a novel biosorbent *Uncaria gambir*: equilibrium, kinetics, and thermodynamic studies. Chem Eng J. 2011;170:145–53.
7. Agboola O, Okoli B, Sanni SE, Alaba PA, Popoola P, Sadiku ER, et al. Synthesis of activated carbon from olive seeds: investigating the yield, energy efficiency, and dye removal capacity. SN Appl Sci. 2018;1(1):85.
8. Hajeeth T, Sudha PN, Kumar V. Removal of Cr (VI) from aqueous solution using graft copolymer of cellulose extracted from sisal fibre with acrylic acid monomer. Cellul Chem Technol. 2015;49:891–900.
9. Odunlami OA, Agboola O, Odiakaose EO, Olabode OO, Babalola O, Abatan OG, Owoicho I. Treatment of contaminated water from Niger Delta oil fields with carbonized sisal fibre doped with nanosilica from ofada rice husk. J Ecol Eng. 2022;23(9):297–308.
10. Belo CR, Cansado IP, Mourão PA. Synthetic polymers blend used in the production of high activated carbon for pesticides removals from liquid phase. Environ Technol. 2017;38(3):285–96.
11. Thadathil A, Pradeep H, Joshy D, Ismail YA, Periyat P. Polyindole and polypyrrole as a sustainable platform for environmental remediation and sensor applications. Mater Adv. 2022;3(7):2990–3022.
12. Saravanan R, Sacari E, Gracia F, Khan MM, Mosquera E, Gupta VK. Conducting PANI stimulated ZnO system for visible light photocatalytic degradation of coloured dyes. J Mol Liq. 2016;221:1029–33.
13. Obulapuram PK, Arfin T, Mohammad F, Khiste SK, Chavali M, Albalawi AN, Al-Lohedan HA. Adsorption, equilibrium isotherm, and thermodynamic studies towards the removal of reactive orange 16 dye using Cu(I)-polyaniline composite. Polymers. 2021;13(20):3490.
14. Kanwal F, Rehman R, Anwar J, Saeed M. Removal of lead(II) from water by adsorption on novel composites of polyaniline with maize bran, wheat bran and rice bran. Asian J Chem. 2013;25:2399–404.
15. Kanwal F, Rehman R, Mahmud T, Anwar J, Ilyas R. Isothermal and thermodynamical modeling of chromium (III) adsorption by composites of polyaniline with rice husk and saw dust. J Chil Chem Soc. 2012;57:1058–63.
16. Zare EN, Motahari A, Sillanpää M. Nanoadsorbents based on conducting polymer nanocomposites with main focus on polyaniline and its derivatives for removal of heavy metal ions/dyes: a review. Environ Res. 2018;162:173–95.
17. Chen H, Yada R. Nanotechnologies in agriculture: new tools for sustainable development. Trends Food Sci Technol. 2011;22(11):585–94.
18. Khajeh M, Laurent S, Dastafkan K. Nanoadsorbents: classification, preparation, and applications (with emphasis on aqueous media). Chem Rev. 2013;113(10):7728–68.
19. de Oliveira AD, Beatrice CAG. Polymer nanocomposites with different types of nanofiller. In: Subbarayan S, editor. Nanocomposites. Rijeka: IntechOpen; 2018.
20. Lei M, Yang L, Shen Y, Yang L, Sun J. Efficient adsorption of anionic dyes by ammoniated waste polyacrylonitrile fiber: mechanism and practicability. ACS Omega. 2021;6(30):19506–16.
21. Badawi AK, Zaher K. Hybrid treatment system for real textile wastewater remediation based on coagulation/flocculation, adsorption and filtration processes: performance and economic evaluation. J Water Process Eng. 2021;40: 101963.
22. Wang Y, Chen R, Dai Z, Yu Q, Miao Y, Xu R. Facile preparation of a polypyrrole modified Chinese yam peel-based adsorbent: characterization, performance, and application in removal of Congo red dye. RSC Adv. 2022;12(15):9424–34.
23. Shaki H. Evaluation of removal of acid dyes using PAM-FeSO$_4$ hybrid polymer as flocculant. Pigm Resin Technol. 2023;52(3):302–9.
24. Teklu T, Wangatia LM, Alemayehu E. In situ deposition of polyaniline onto sisal fibers and removal efficiency for chromium (VI) from aqueous solution: structure and adsorption studies. J Appl Surf Interfaces. 2018;3:1–9.
25. Lyu W, Yu M, Feng J, Yan W. Highly crystalline polyaniline nanofibers coating with low-cost biomass for easy separation and high efficient removal of anionic dye ARG from aqueous solution. Appl Surf Sci. 2018;458:413–24.
26. Sood M, Deepak D, Gupta VK. Tensile properties of sisal fiber/recycled polyethylene (high density) composite: effect of fiber chemical treatment. Mater Today Proc. 2018;5(2, Part 1):5673–8.
27. Adugna Ayalew A, Fenta Wodag A. Characterization of chemically treated sisal fiber/polyester composites. J Eng. 2022. https://doi.org/10.1155/2022/8583213.
28. Zhou Y, Wang T, Zhi D, Guo B, Zhou Y, Nie J, et al. Applications of nanoscale zero-valent iron and its composites to the removal of antibiotics: a review. J Mater Sci. 2019;54(19):12171–88.
29. Adly A, Mostafa NG, Elawwad A. Adsorption of phosphorus onto nanoscale zero-valent iron/activated carbon: removal mechanisms, thermodynamics, and interferences. Water Reuse. 2022;12(1):111–30.
30. Wang Z, Wu X, Luo S, Wang Y, Tong Z, Deng Q. Shell biomass material supported nano-zero valent iron to remove Pb(2+) and Cd(2+) in water. R Soc Open Sci. 2020;7(10): 201192.
31. Painter P, Coleman M. Fundamentals of polymer science: an introductory text. London: Routledge; 2019.
32. Ravikumar KVG, Dubey S, Pulimi M, Chandrasekaran N, Mukherjee A. Scale-up synthesis of zero-valent iron nanoparticles and their applications for synergistic degradation of pollutants with sodium borohydride. J Mol Liq. 2016;224:589–98.
33. Çuhadar Ç. Production and characterization of activated carbon from hazelnut shell and hazelnut husk. Ankara: Middle East Technical University; 2005.

34. Yuan Y, An Z, Zhang R, Wei X, Lai B. Efficiencies and mechanisms of heavy metals adsorption on waste leather-derived high-nitrogen activated carbon. J Clean Prod. 2021;293: 126215.

35. Agboola O, Maree JP, Mbaya KK. Characterization and performance of nanofiltration membranes. Environ Chem Lett. 2014;12:241–55.

36. Subramanyam B, Das A. Linearised and non-linearised isotherm models optimization analysis by error functions and statistical means. J Environ Health Sci Eng. 2014;12:92.

37. Kumar P, Saini M, Singh M, Chhillar N, Brijnandan S, Dehiya B, Kishor K, et al. Micro-plasma assisted synthesis of ZnO nanosheets for the efficient removal of Cr6+ from the aqueous solution. Crystals. 2020;11(1):2.

38. Darweesh MA, Elgendy MY, Ayad MI, Ahmed AM, Elsayed NMK, Hammad WA. Adsorption isotherm, kinetic, and optimization studies for copper (II) removal from aqueous solutions by banana leaves and derived activated carbon. S Afr J Chem Eng. 2022;40:10–20.

39. Kalam S, Abu-Khamsin SA, Kamal MS, Patil S. Surfactant adsorption isotherms: a review. ACS Omega. 2021;6(48):32342–8.

40. Xu D, Tan X, Chen C, Wang X. Removal of Pb(II) from aqueous solution by oxidized multiwalled carbon nanotubes. J Hazard Mater. 2008;154(1):407–16.

41. Gebretsadik T, Wangatia L, Alemayehu E. Removal of Pb(II) from aqueous media using adsorption onto polyaniline coated sisal fibers. J Vinyl Addit Technol. 2018;25:189–97.

42. Kaliannan D, Palaninaicker S, Palanivel V, Mahadeo MA, Ravindra BN, Jae-Jin S. A novel approach to preparation of nano-adsorbent from agricultural wastes (*Saccharum officinarum* leaves) and its environmental application. Environ Sci Pollut Res Int. 2019;26(6):5305–14.

43. Saha D, Grappe HA. 5—Adsorption properties of activated carbon fibers. In: Chen JY, editor. Activated carbon fiber and textiles. Oxford: Woodhead Publishing; 2017. p. 143–65.

44. Revellame ED, Fortela DL, Sharp W, Hernandez R, Zappi ME. Adsorption kinetic modeling using pseudo-first order and pseudo-second order rate laws: a review. Clean Eng Technol. 2020;1: 100032.

45. Wu F-C, Tseng R-L, Juang R-S. Characteristics of Elovich equation used for the analysis of adsorption kinetics in dye-chitosan systems. Chem Eng J. 2009;150(2):366–73.

46. Lan X, Jiang X, Song Y, Jing X, Xing X. The effect of activation temperature on structure and properties of blue coke-based activated carbon by CO$_2$ activation. Green Process Synth. 2019;8(1):837–45.

47. Ben Nasr J, Hamdi N, Elhalouani F. Characterization of activated carbon prepared from sludge paper for methylene blue adsorption. J Mater Environ. 2017;8:1960–7.

48. Shokry H, Elkady M, Hamad H. Nano activated carbon from industrial mine coal as adsorbents for removal of dye from simulated textile wastewater: operational parameters and mechanism study. J Market Res. 2019;8(5):4477–88.

49. Zakaria R, Jamalluddin NA, Abu Bakar MZ. Effect of impregnation ratio and activation temperature on the yield and adsorption performance of mangrove based activated carbon for methylene blue removal. Results Mater. 2021;10: 100183.

50. Maneerung T, Liew J, Dai Y, Kawi S, Chong C, Wang C-H. Activated carbon derived from carbon residue from biomass gasification and its application for dye adsorption: kinetics, isotherms and thermodynamic studies. Bioresour Technol. 2016;200:350–9.

51. Lu X, Jiang J, Sun K, Xie X. Preparation and characterization of sisal fiber-based activated carbon by chemical activation with zinc chloride. Bull Korean Chem Soc. 2014;35:103–10.

52. Joulazadeh M, Navarchian A. Alcohol sensibility of one-dimensional polyaniline and polypyrrole nanostructures. IEEE Sens J. 2015;15:1697–704.

53. Ali J, Bakhsh EM, Hussain N, Bilal M, Akhtar K, Fagieh TM, et al. A new biosource for synthesis of activated carbon and its potential use for removal of methylene blue and eriochrome black T from aqueous solutions. Ind Crops Prod. 2022;179: 114676.

54. Yasmeen S, Kanti Kabiraz M, Saha B, Rakibul Qadir M, Abdul Gafur M, Md. Masum S. Chromium (VI) ions removal from tannery effluent using chitosan-microcrystalline cellulose composite as adsorbent. Int Res J Pure Appl Chem. 2015;10(4):1–14.

55. Rahaman MH, Islam MA, Islam MM, Rahman MA, Alam SMN. Biodegradable composite adsorbent of modified cellulose and chitosan to remove heavy metal ions from aqueous solution. Curr Res Green Sustain Chem. 2021;4: 100119.

56. Thommes M, Kaneko K, Neimark AV, Olivier JP, Rodriguez-Reinoso F, Rouquerol J, Sing KSW. Physisorption of gases, with special reference to the evaluation of surface area and pore size distribution (IUPAC technical report). Pure Appl Chem. 2015;87(9–10):1051–69.

57. Xing X, Alharbi NS, Ren X, Chen C. A comprehensive review on emerging natural and tailored materials for chromium-contaminated water treatment and environmental remediation. J Environ Chem Eng. 2022;10(2): 107325.

58. Al-Thani NJ, Bhadra J, Abdulmalik D, Al-Qaradawi I, Alashraf A, Madi NK. Positron annihilation study on polyaniline nanocomposite used for Pb(II) ion removal. Desalin Water Treat. 2016;57(56):27374–85.

59. Molina-Calderón L, Basualto-Flores C, Paredes-García V, Venegas-Yazigi D. Advances of magnetic nanohydrometallurgy using superparamagnetic nanomaterials as rare earth ions adsorbents: a grand opportunity for sustainable rare earth recovery. Sep Purif Technol. 2022;299: 121708.

60. Senthil Kumar P, Ramalingam S, Senthamarai C, Niranjanaa M, Vijayalakshmi P, Sivanesan S. Adsorption of dye from aqueous solution by cashew nut shell: studies on equilibrium isotherm, kinetics and thermodynamics of interactions. Desalination. 2010;261(1):52–60.

61. Aljeboree AM, Alshirifi AN, Alkaim AF. Kinetics and equilibrium study for the adsorption of textile dyes on coconut shell activated carbon. Arab J Chem. 2017;10:S3381–93.

62. Ramutshatsha-Makhwedzha D, Mavhungu A, Moropeng ML, Mbaya R. Activated carbon derived from waste orange and lemon peels for the adsorption of methyl orange and methylene blue dyes from wastewater. Heliyon. 2022;8(8): e09930.

63. Mihai S, Bondarev A, Călin C, Sîrbu E-E. Adsorbent biomaterials based on natural clays and orange peel waste for the removal of anionic dyes from water. Processes. 2024;12(5):1032.

64. Wang P, Cao M, Wang C, Ao Y, Hou J, Qian J. Kinetics and thermodynamics of adsorption of methylene blue by a magnetic graphene-carbon nanotube composite. Appl Surf Sci. 2014;290:116–24.

65. Yao Y, Miao S, Yu S, Ping Ma L, Sun H, Wang S. Fabrication of Fe$_3$O$_4$/SiO$_2$ core/shell nanoparticles attached to graphene oxide and its use as an adsorbent. J Colloid Interface Sci. 2012;379(1):20–6.

66. Neolaka YAB, Riwu AAP, Aigbe UO, Ukhurebor KE, Onyancha RB, Darmokoesoemo H, Kusuma HS. Potential of activated carbon from various sources as a low-cost adsorbent to remove heavy metals and synthetic dyes. Results Chem. 2023;5: 100711.

67. Akinyemi FA, Agboola O, Oladokun O, Alagbe EE, Sadiku R. Surface modification and integration of organic/inorganic additives into the matrix of the membrane: the governing interaction mechanisms of dye adsorption on adsorptive membranes. J Membr Sci Res. 2024. https://doi.org/10.22079/jmsr.2023.2008829.1623.

68. Raji Z, Karim A, Karam A, Khalloufi S. Adsorption of heavy metals: mechanisms, kinetics, and applications of various adsorbents in waste-water remediation—a review. Waste. 2023;1(3):775–805.

69. Hoang AT, Kumar S, Lichtfouse E, Cheng CK, Varma RS, Senthilkumar N, et al. Remediation of heavy metal polluted waters using activated carbon from lignocellulosic biomass: an update of recent trends. Chemosphere. 2022;302: 134825.

70. Xue S, Hu Y, Wan K, Miao Z. Exploring humic acid as an efficient and selective adsorbent for lead removal in multi-metal coexistence systems: a review. Separations. 2024;11(3):80.

71. Wang B, Lan J, Bo C, Gong B, Ou J. Adsorption of heavy metal onto biomass-derived activated carbon: review. RSC Adv. 2023;13(7):4275–302.

Discover